Power system resilience support from heat-pump equipped houses — thermal comfort consequence for various room priority strategies

Energy Conversion and Management: X 29 (2026) 101436

Contents lists available at ScienceDirect

Energy Conversion and Management: X

journal homepage: www.sciencedirect.com/journal/energy-conversion-and-management-x

Power system resilience support from heat-pump equipped houses — thermal comfort consequence for various room priority strategies

Sindhu Kanya Nalini Ramakrishna *, Torbjörn Thiringer, Peiyuan Chen

Division of Electric Power Engineering, Chalmers University of Technology, Gothenburg, 41296, Sweden

ARTICLE INFO

Keywords:
Flexibility quantification
Space heating
Heat pumps
Multi-room house

ABSTRACT

Swedish single-family houses equipped with heat pumps could serve as valuable flexible resources to support the power system in situations of severe power shortages. Hence, to quantify the flexibility potential by maintaining different temperatures in a multi-room house, a detailed model of a house equipped with a variable speed heat pump is developed. In this study, flexibility is defined as a reduction in the electric power consumption of a heat pump, relative to the electric power consumption when maintaining 20 °C throughout the house.

A flexibility of 100% is provided for 5 h, when all rooms reduce thermal comfort equally to about 16 °C, at an outdoor temperature of −5 °C. The same flexibility can also be provided by heating only a smaller area, such as a better insulated bedroom, which is 8% of the total floor area, to 17.5 °C, while ensuring that the temperatures in the other rooms do not fall below 10 °C. After the first five hours, the flexibility decreases from 100% to 47% and 57%, respectively, in the above cases, for as long as the flexibility required. The impact of offering various levels of flexibility in relation to thermal comfort is demonstrated and quantified in this article.

1. Introduction

In Sweden, winter represents a critical period for the power system as it is sometimes operated nearly close to its limits. Colder weather conditions coupled with a loss of a major power plant or cyber attacks on the control system of power plants and transmission systems could lead to severe power deficit conditions [1].

To prevent a collapse of the power system during such power-deficit situations, the available electric power could be rationed [2]. In such a scenario, identifying the loads with the high electric power consumption, as well as the loads that could contribute to resilience, helps network operators take suitable actions in case of dramatic power-deficit situations.

Electric energy consumption is the highest in the residential and service sector in Sweden [3]. Furthermore, in the residential sector, the electric energy consumption is the highest in single-family houses [4]. About 65% of these houses use electricity for heating [5], with the majority equipped with heat pumps. In houses equipped with heat pumps, about 50% of this consumption is attributed to space and water heating [6]. Furthermore, energy efficiency measures are an important ongoing process with a significant impact on the power system. One important process is that, fixed-speed heat pumps are being replaced with new variable speed heat pumps, which have high controllability. Thus, single-family houses equipped with variable speed heat pumps could serve as valuable resources to reduce the electric power consumption during severe power shortage situations.

The flexibility potential of space heating in about a million Swedish single-family houses equipped with heat pumps, to support the power system during severe power deficit conditions is quantified in [7]. A potential of 1.6 GW is estimated at −5 °C outdoor temperature, with the consequence of compromising thermal comfort. In [7], the indoor temperature is reduced to the same value throughout a house. Ref. [7] also contained interviews from households revealing that the respondents had different temperature preferences for different rooms. The potential for load reduction while maintaining different indoor temperatures in various rooms of a house is yet to be investigated.

Johnson et al. [8] deals with the modelling of heat pumps and a physics-based multi-zone model of a building to generate the profiles of electric power consumption by heat pumps. In [8], heat pumps are of the traditional fixed-speed type, which were fully dominating half a decade ago. However, today, as mentioned above, variable-speed heat pumps are becoming dominant. Khatibi et al. [9] presents a hierarchical model-based scheme to offer flexibility, considering a multi-zone building model to control temperatures in different zones of a building. In this article, an air-to-air heat pump is used. It would

* Corresponding author.
E-mail address: kanya@chalmers.se (S.K. Nalini Ramakrishna).

https://doi.org/10.1016/j.ecmx.2025.101436
Received 21 October 2025; Received in revised form 28 November 2025; Accepted 1 December 2025
Available online 4 December 2025

Table 1
Summary of literature review undertaken.

Reference	Thermal model of building	Heat pump model
[8]	2R3C model-floor, walls and roof	Empirical
[9]	Grey box	✗
[10]	Grey box	✗
[11]	Grey box	✗
[12]	IDA ICE	✗
[13]	TRANSYS	Empirical
[14]	Carnot tool box	Empirical
[15]	Grey box	✗
[16]	Grey box	✗
[17]	Grey box	✗
[18]	Each zone- 3R1C model	✗

be interesting to study heat pumps with water-based heating systems which are typical in Sweden.

Golmohamadi et al. [10] involves modelling and temperature control in multiple rooms according to occupancy, to optimise the electric power consumption of a heat pump. Golmohamadi et al. [11] also deals with unlocking the flexibility potential based on occupancy, by accounting for thermal dynamics in multiple rooms of a Danish test house, using an economic model predictive control. The flexibility potential in a single family house in Norway is investigated by modelling and controlling temperatures in multiple rooms, using predictive rule-based control in [12]. The annual savings in electric energy using a heat pump compared to the boiler system is quantified by simulating a terraced house in Wales with multiple temperature zones in article [13]. In the above articles, a buffer tank is used in space heating, which is typically absent in Swedish single-family houses. Thus, the impact on thermal comfort will be more noticeable in Swedish single-family houses, which requires further investigation. Furthermore, the heat pump models incorporated in these studies are not dealt in detail.

Hua et al. [14] presents an integrated demand response method, to reduce operational cost by selecting various indoor temperature set points for different rooms, for a space heating system involving an air source heat pump and district heating in an educational building. Articles [15,16] deal with the operational optimisation of a heat pump, battery, and rooftop solar to reduce peak electricity demand and operational costs, while ensuring thermal comfort in different rooms of a building, respectively. Frahm et al. [17] presents a multizone price storage control, to reduce the operating cost of a space heating system equipped with a heat pump, by accounting for the thermal satisfaction of the occupants, without the need for a building model. Verdugo et al. [18] deals with controlling temperatures in different rooms with the objective of reducing operational costs for a microgrid involving heat pumps and battery storages. In the articles dealt with above, even though buildings with multiple rooms are modelled, heat pump models are not dealt with in detail and lack the information on operational limitations. Incorporating these limitations is an important aspect, as it has an impact on the electric power consumption by heat pumps under various operating conditions.

A summary of the literature review is presented in Table 1. In these articles, the thermal models of multi-room houses are not fully transparent and reproducible. For example, in [14], the thermal model of the house is not described in detail. In Refs. [12,18] the values of the thermal mass associated with the different components of the building are missing. Articles [9–11,15–17] use grey box modelling to identify building parameters. Thus, the models presented are not fully transparent and reproducible. Furthermore, the heat pump models incorporated in these studies [8–18] are either empirical or not described and lack information on operating limitations under various operating conditions.

Missing in the scientific literature is a detailed model of a multi-room house equipped with a variable-speed heat pump. In addition, all the above articles deal with either reducing the operational cost or with flexibility studies for normal demand side management. They do not deal with supporting a power system with severe power deficit conditions, which then leaves a research gap to fill.

In this study, flexibility is defined as a reduction in the electric power consumption of a heat pump, relative to the electric power consumption while maintaining 20 °C in a house. Thus, with this background, the main contributions of this article are as follows.

- Quantification and comparison of the flexibility potential by maintaining different indoor temperatures in various rooms of a house, to support the power system during severe power deficit conditions.
- A detailed thermal model of a multi-room house considering construction materials, infiltration losses and the heat recovery is presented. Furthermore, the model also includes a detailed model of an air source heat pump considering the operational limitations at various operating conditions.
- The effectiveness of the proposed space heating controller to control different temperatures in a multi-room house, at different conditions is demonstrated.

2. Method

2.1. Air source heat pump model

To estimate the flexibility potential, it is important to know the performance of a heat pump under various operating conditions. The performance of heat pump is estimated using the vapour compression heat pump cycle.

Fig. 1 illustrates a vapour compression heat pump cycle, including its associated components, along with the corresponding states on a pressure–enthalpy diagram. The procedure for estimating the power consumed by the compressor and COP is as follows [7]:

- The refrigerant mass flow rate $\dot{m}$, is determined using

$$\dot{m} = \frac{V_{dis}\rho_s f \eta_{vol}}{10^6} \tag{1}$$

  where V_{dis} denotes the compressor displacement volume in $\left(\frac{\text{cc}}{\text{rev}}\right)$, ρ_s is the refrigerant's density at suction in $\left(\frac{\text{kg}}{\text{m}^3}\right)$, f represents the frequency in (Hz), and η_{vol} is the compressor's volumetric efficiency.
- Using efficiencies related to energy flows to a compressor [19], the required electric power input to the compressor can be expressed as

$$P_{comp} = \frac{\dot{m}(h_2 - h_1)}{\eta_{isent,speed}} \tag{2}$$

  Here, h denotes the enthalpy at the state specified by the subscript. The term $\eta_{isent,speed}$ refers to the overall isentropic efficiency at various compressor speeds for a given compression ratio and is evaluated following the approach described in [20].
- The coefficient of performance (COP) for a heat pump is expressed as

$$COP = \frac{\dot{m}(h_2 - h_3)}{P_{comp}} \tag{3}$$

In modern air source heat pumps, the operating range at low outdoor temperatures is extended and performance is increased by employing enhanced vapour injection (EVI) technology.

Figs. 2 and 3 illustrate vapour injection in a heat pump and on a pressure–enthalpy diagram, respectively. In this configuration, vapour is injected at a temperature that lies between the evaporator and condenser temperatures. A portion of the condensed refrigerant, with a mass flow rate $\dot{m}$ after being subcooled in the condenser, is directed to a heat exchanger. The remaining portion, with a mass flow rate $\dot{m}_{inj}$, first passes through an expansion valve and then enters the economiser's

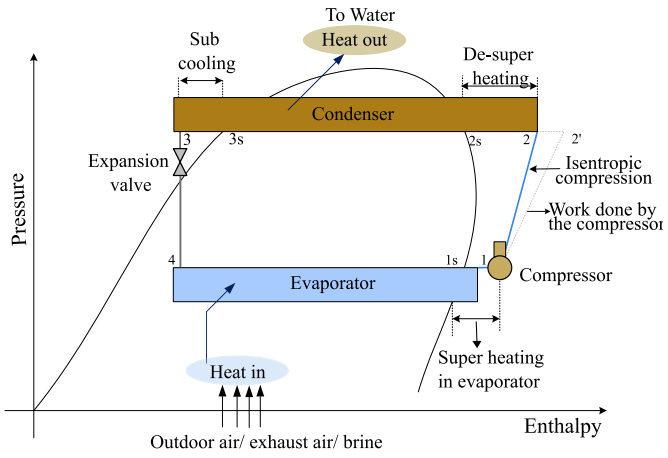

Fig. 1. Heat pump model [7].

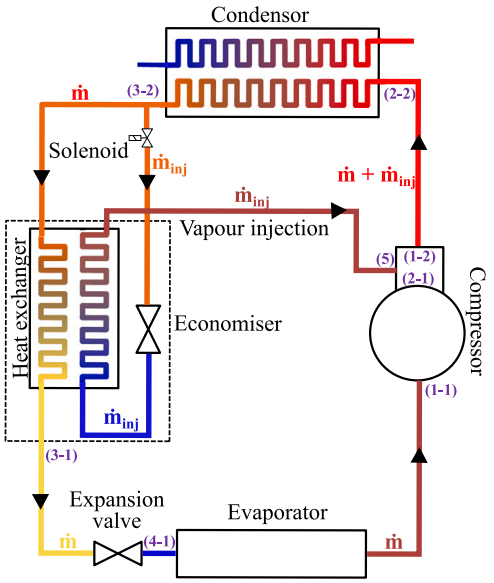

Fig. 2. Vapour injection in scroll compressors [21].

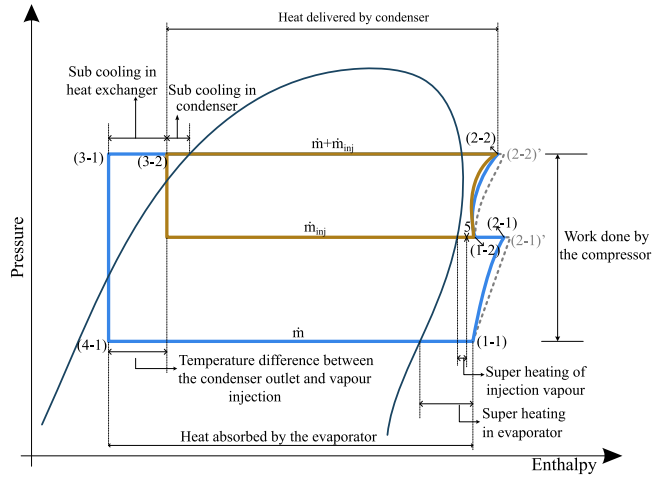

Fig. 3. Vapour compression heat pump cycle with vapour injection [22].

heat exchanger, as illustrated in Fig. 2. Inside the economiser's heat exchanger, the heat released by $\dot{m}$ during sub cooling is transferred to $\dot{m}_{inj}$. As a result, $\dot{m}_{inj}$ is superheated and injected into the compressor through an injection port. Consequently, the compressor performs compression in two stages. The first stage compresses the superheated vapour exiting the evaporator. The second stage compresses the injected superheated vapour and the vapour discharged from the first compression. The different thermodynamic states of the refrigerant are indicated in both Figs. 2 and 3 in parentheses.

A comprehensive method for estimating the COP of a heat pump with vapour injection is provided in [23]. The main aspects involved in modelling such a heat pump are outlined briefly below:

- The mass flow rate of the injected vapour, $\dot{m}_{inj}$, is determined from the energy balance in the economiser and can be expressed as

$$\dot{m}_{inj} = \frac{\dot{m}(h_{3-2} - h_{3-1})}{(h_5 - h_{3-2})} \tag{4}$$

  Here, h denotes the specific enthalpy at the state indicated by the subscript.
- The specific enthalpy at state 1–2, h_{1-2}, is determined using the energy balance equation at the compressor's vapour injection port and can be expressed as

$$\dot{m}_{inj}(h_{1-2} - h_5) = \dot{m}(h_{2-1} - h_{1-2})$$
$$h_{1-2} = \frac{\dot{m}h_{2-1} + \dot{m}_{inj}h_5}{(\dot{m} + \dot{m}_{inj})} \tag{5}$$

- The electric power consumption of the compressor is determined as

$$P_{comp} = \frac{\dot{m}(h_{2-1} - h_{1-1}) + (\dot{m} + \dot{m}_{inj})(h_{2-2} - h_{1-2})}{\eta_{isent}} \tag{6}$$

  where η_{isent} denotes the isentropic efficiency. Its variation under different operating conditions is determined as outlined in [20].
- The COP of a heat pump is expressed as

$$COP = \frac{(\dot{m} + \dot{m}_{inj})(h_{2-2} - h_{3-2}))}{P_{comp}} \tag{7}$$

2.2. Thermal model of a house with multiple rooms

In [8], as shown in Table 1, a 2R3C model is used to represent each wall, roof, and floor. In [18], the thermal capacitances of the internal walls are neglected as the storage capacity is limited due to the high thermal conductivity. Furthermore, the thermal mass of the external envelope is combined with the thermal mass of the indoor air to reduce the number of variables in the model. Finally, each zone is represented using a 3R1C model.

To better capture the thermal dynamics of the house, the thermal model used in this study strikes a balance between the detailed approach in [8] and the simple model in [18]. This is because, in addition to the building's thermal model, the study also includes a detailed model of the heat pump, the design of the indoor temperature controller, and the procedure for estimating the water supply temperature to the radiators in each zone to meet different heating requirements, which are missing in the literature. The thermal model adopted in this study is explained below.

Based on the construction materials of the building, the thermal resistance and thermal capacitance of the external envelope (external walls and roof), internal walls and floor are computed. Each component of the building (walls, roof, and floor) is composed of several materials. The total thermal resistance and thermal capacitance of each component [24] are computed as

$$R_x = \sum_{i=1}^{n} \frac{t_i}{G_i\ A_x} \tag{8}$$

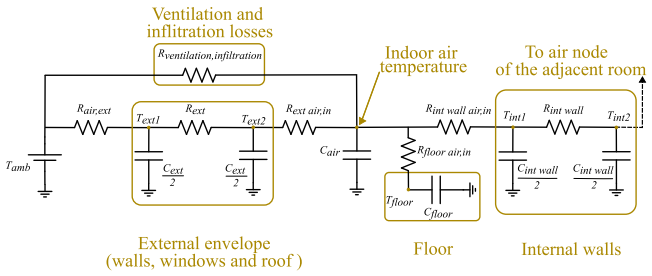

Fig. 4. Thermal model of one zone in a multi-zone thermal model.

$$C_x = \sum_{i=1}^{n} \rho_i \, C_{p_i} \, t_i \, A_x \tag{9}$$

where $x \in \{\text{external walls, roof, internal walls, floor}\}$, i corresponds to various materials in each component of the building, t_i is the thickness of the material in (m), G_i is the thermal conductivity in $\left(\frac{\text{W}}{\text{mK}}\right)$, A_x is the area of the building component in (m^2), ρ_i is the density in $\left(\frac{\text{Kg}}{\text{m}^3}\right)$ and Cp_i is the specific heat capacity in $\left(\frac{\text{J}}{\text{kg K}}\right)$.

The thermal resistance of the external envelope is obtained from the parallel combination of the thermal resistances of windows, doors, external walls, and the roof. The thermal mass of the external envelope is obtained by summing the associated thermal masses together.

In addition, the heat loss coefficients due to mechanical ventilation and infiltration [7] are computed as

$$R_{ventilation,infiltration} = \left(\frac{\rho_{air} C_{p,air}}{1000} \left((1 - \eta_{vent}) V_{vent} A_{floor} + V_{infil} A_{ext} \right) \right)^{-1} \tag{10}$$

where, ρ_{air} is the density of air in $\left(\frac{\text{Kg}}{\text{m}^3}\right)$ and $C_{p,air}$ is the specific heat capacity of air in $\left(\frac{\text{J}}{\text{Kg K}}\right)$, η_{vent} is the efficiency of the heat recovery unit, V_{vent} and V_{infil} are the ventilation rates for sanitary ventilation and infiltration, respectively, in $\left(\frac{1}{\text{s}\cdot\text{m}^2}\right)$. A_{floor} is the heated floor area and A_{ext} is the exterior surface area of the building envelope in (m^2) (excluding windows and doors).

The thermal mass of the indoor air including the furnishings [13, 25,26] is computed as

$$C_{air} = ZM \left(\rho_{air} \, C_{p,air} \, V_{room} \right) \tag{11}$$

where, ZM is the zone capacity multiplier factor, which accounts for the furnishings contributing to the internal thermal mass. V_{room} is the volume of air in the room in (m^3).

Fig. 4 shows the thermal model of one zone in a multi-zone model of a house. The external envelope and the internal walls are modelled using a 1R2C network.

The heat loss coefficient due to ventilation and infiltration is modelled as a resistance [24]. The thermal resistances ($R_{air,ext}$, $R_{ext\ air,in}$, $R_{int\ wall\ air,in}$, $R_{floor\ air,in}$) due to convection and radiation from the surfaces of walls and floors are also taken into account [24], as seen in Fig. 4.

2.3. Radiator model

The thermal output from the radiators is modelled as

$$Q_{heat} = Q_{std} \left(\frac{\Delta T_{act}}{\Delta T_{std}} \right)^{n} \tag{12}$$

Q_{std} and ΔT_{std} represent the total heat output of the radiators and reference temperature at standard conditions (i.e., at 55 °C supply temperature, 45 °C return temperature and 20 °C room temperature) respectively. The term n refers to the exponent characteristic of the radiator. Furthermore, ΔT_{act} is computed as

$$\Delta T_{act} = \begin{cases} \dfrac{T_{supply} - T_{return}}{ln\left(\frac{T_{supply} - T_{room}}{T_{return} - T_{room}}\right)} & \text{if } \left(\dfrac{T_{return} - T_{room}}{T_{supply} - T_{room}}\right) < 0.7 \\ \dfrac{T_{supply} + T_{return}}{2} - T_{room} & \text{Otherwise} \end{cases} \tag{13}$$

where, T_{supply} and T_{return} represent the water supply temperature and return temperature in the radiators respectively. T_{room} represents the room temperature.

2.4. Controller design

A closed loop proportional-integral (PI) controller with an anti-wind up and a feed-forward structure is chosen, to control the main zone's indoor temperature. A rule-based control structure is adopted to control the indoor temperature in the other zones of the building.

The block diagram of the adopted multi-zone temperature controller structure is shown in Fig. 5. From a simplicity point of view, only two zones are represented. This structure can be extended to several zones, with a dedicated PI controller in the main zone.

The design details of the adaptive limiter are shown in Fig. 6. For the rule-based controller, using the thermal model of the zone presented in Fig. 4 as a reference, the desired heat is calculated using the estimated temperatures of the external envelope, internal walls, floor, outdoor temperature and the desired indoor temperature as

$$\begin{aligned} Q_{heat,zp}{}^{**}(t) = -\Bigg(& \frac{T_{amb}(t) - T_{desiredroomzp}(t)}{R_{ventilation,infiltration}} \\ & + \frac{T_{ext2}(t) - T_{desiredroomzp}(t)}{R_{extair,in}} \\ & + \frac{T_{int1}(t) - T_{desiredroomzp}(t)}{R_{intwallair,in}} \\ & + \frac{T_{floor}(t) - T_{desiredroomzp}(t)}{R_{floorair,in}} \Bigg) \end{aligned} \tag{14}$$

Here, p represents the zone number in the house with multiple zones with the rule-based controller. The unlimited output from both the rule-based controller and the PI controller is represented as $Q_{heat,zp}{}^{**}$.

The formulation of the radiator look-up table (LUT) for each zone is based on the radiator model described in Section 2.3. The LUT is generated by computing the thermal output of the radiators for various combinations of water supply and return temperatures, at different indoor air temperatures. This table is constructed for a fixed temperature difference between the water supply and the return temperature in the radiators, indicated by ΔT.

The radiator LUT provides the required water supply temperature based on the desired heat value to be delivered and the actual indoor temperature. Based on the room temperature and the estimated water supply temperature in each zone, the thermal output considering the limitations of the radiators in each zone is estimated $Q_{heat,zp}{}^{*}$.

After estimating the temperature of the water supply to the radiators required in various zones, a maximum value is chosen. Finally, based on the maximum value of the required supply temperature and the average value of the return water temperature obtained from different zones, the required condenser temperature is estimated as

$$T_{cond}{}^{*} = T_{return,average} + \frac{\hat{T}_{supply} * - T_{return,average}}{1 - e^{\frac{-(\hat{T}_{supply}{}^{*} - T_{return,average})}{\Delta T_{log.cond}}}} \tag{15}$$

$\Delta T_{log.cond}$, is the logarithmic temperature difference of the heat exchanger and is assumed to be 4 K.

Based on the condenser temperature, the desired value of heat considering the limitations in the radiators and the source temperature of the heat pump (T_{source}), the heat pump model provides the actual value of heat delivered, the water supply temperature, power consumption by the heat pump including the details on additional electric heating and the speed of the compressor.

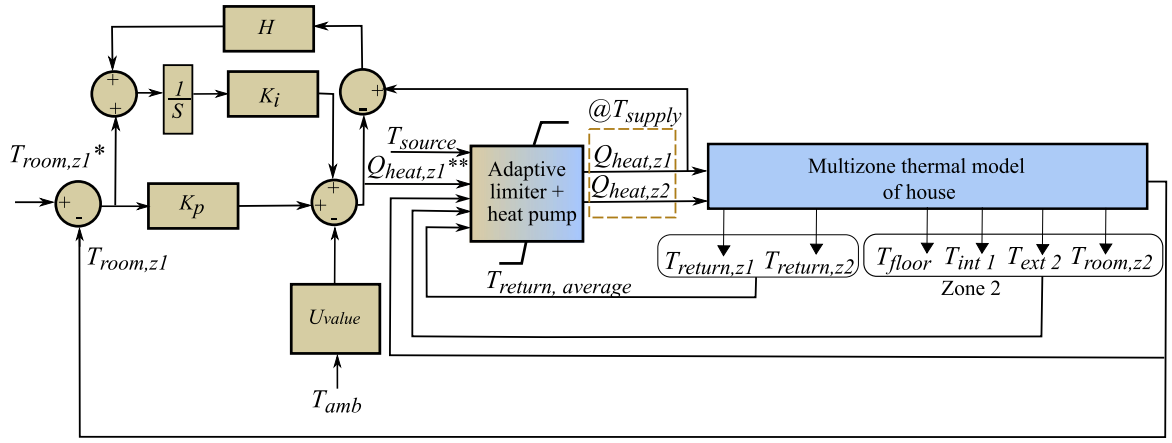

Fig. 5. Multi-zone temperature controller structure.

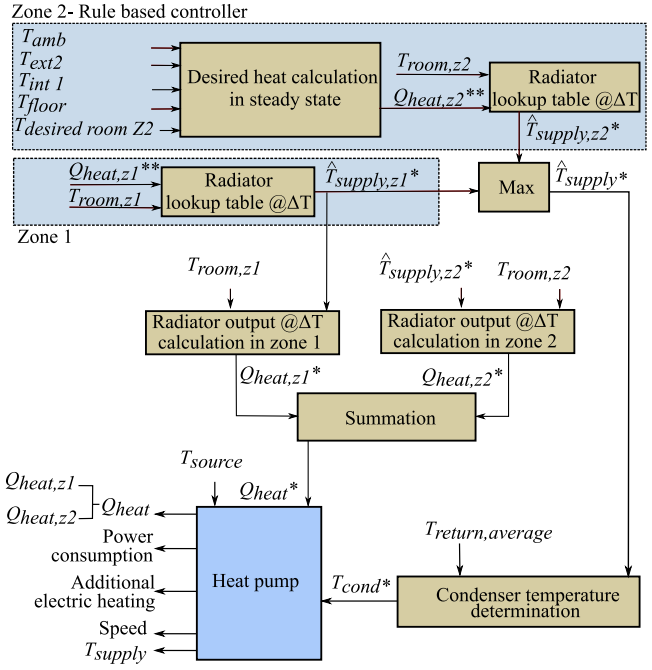

Fig. 6. Adaptive limiter of the proposed multi-zone temperature controller.

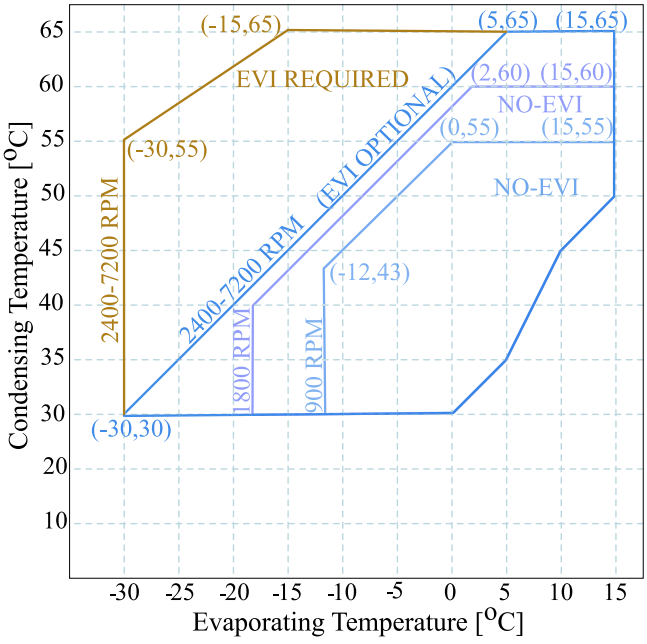

Fig. 7. Compressor operating envelope [27].

3. Case study set up

3.1. Heat pump parameters

Scroll compressors are commonly used in residential applications. Hence, the compressor in the air source heat pump under study is assumed to be equipped with 'ZPV030' Copeland's variable speed scroll compressor, having an electric rating of 3 kW. The compressor displacement volume is 30 $\left(\frac{cc}{rev}\right)$ and the operating envelope is shown in Fig. 7. Refrigerant R410a is used and the rating of the additional electric heater is 3 kW.

The temperature drop between the outdoor ambient temperature and the evaporator in the air source heat pump is set to 8 °C [28].

3.2. Building parameters

The floor plan of the house considered for the analysis is based on a study in [29] and is shown in Fig. 8. The area of all the doors represented is 2.3 m^2. The total area dedicated to windows in each room and the details of the radiators considered for the analysis are tabulated in Table 2. The ceiling height of the building is 2.5 metres and the roof area is equal to the total floor area of the house.

Table 2
Area of the windows and type of radiator used in each room of the house considered for the analysis.

Room	Total window area (m^2)	Radiator type	Number of radiators
Bedroom 1	3.1	PURMO C 33 400 × 1000	2
Bedroom 2	1.9	PURMO C 33 400 × 1200	1
Bedroom 3	1.9	PURMO C 33 400 × 1200	2
Bath room and laundry	0.3	PURMO C 33 400 × 1000	2
Living room and kitchen	9.18	PURMO C 33 400 × 2000	4

The specifications and properties of the construction materials used in the exterior walls, roof, internal walls and the floor are tabulated in

Table 3
Specifications of building construction materials used in various building components [29].

External walls		Roof		Internal walls		Floor	
Materials	Thickness (m)	Materials	Thickness (m)	Materials	Thickness (m)	Materials	Thickness (m)
Timber stud	0.246	Mineral wool	0.35	Drywall	0.013	Concrete	0.1
Particleboard	0.013	Drywall	0.013	Particleboard	0.070	–	–
Drywall	0.013	–	–	Drywall	0.013	–	–

Table 4
Properties of the building's construction materials considered for the analysis [29].

Material	Timber stud	Particle board	Drywall	Mineral wool	Concrete
Density $\left(\frac{kg}{m^3}\right)$	87	600	900	40	2300
Heat capacity $\left(\frac{J}{KgK}\right)$	961	2300	1100	800	800
Thermal conductivity $\left(\frac{W}{mK}\right)$	0.045	0.14	0.22	0.042	1.7

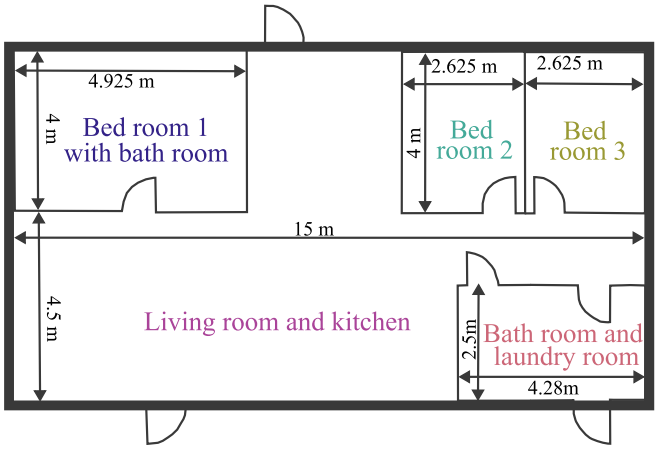

Fig. 8. Floor plan of the house considered for the analysis [29].

Tables 3 and 4, respectively. The thermal resistances for the door and windows are set to 1.4 $\left(\frac{W}{m^2K}\right)$.

In this study a ventilation rate of 0.35 $\left(\frac{1}{s \cdot m^2}\right)$ and an infiltration rate of 0.6 $\left(\frac{1}{s \cdot m^2}\right)$ are used. Based on Ref. [24], the thermal resistance due to convection and radiation on the surfaces of the external walls exposed to outdoor air ($R_{air,ext}$) is set at 25 $\left(\frac{W}{m^2K}\right)$. The thermal resistance due to convection and radiation on the surfaces of the walls and the floor facing the indoor air ($R_{intwallair,in}$, $R_{floorair,in}$) is set to 7.7 $\left(\frac{W}{m^2K}\right)$ [24].

Based on the Ref. [25,26], the zone capacity multiplier factor is set to 25 for the living room and 15 each for the bedrooms and the bathroom.

The indoor temperature is set to be 20 °C during normal conditions, based on a study in [30]. An outdoor ambient temperature of −5 °C is considered as it is a common winter temperature in southern half of Sweden, where the electricity demand is typically high.

3.3. Building specifications for the thermal model

Based on the floor plan of the house presented in Fig. 8, five thermal zones are modelled. Three zones dedicated to three bedrooms and one each for the living room and the bathroom. The living room is set to be the main zone as it is larger in area compared to the other zones, and hence a PI controller is used in this zone to control the indoor temperature. The indoor temperature in the other four zones is controlled using rule-based controllers as explained in Section 2.4.

The thermal model of the house with five zones is shown in Fig. 9. The heat output from the radiators is injected into the indoor temperature node in each zone.

3.4. Case study description

An interview study was conducted by RISE (Research Institutes of Sweden) with single-family home owners equipped with heat pumps in [7]. The main aim was to obtain nuanced information regarding the households' perspective of offering flexibility by compromising the thermal comfort to support the power system under severe power deficit conditions.

The lowest indoor temperature stated in the interviews was 15 °C. Furthermore, the study revealed that households had different preferences for indoor temperatures, while offering flexibility to support the grid in conditions of severe power shortages. Most of the interviewees preferred to have colder bedrooms and a warmer living room. In addition, some of them were positive about shutting down the heating system in storage rooms, garages, and bedrooms while having a warmer living room.

Thus, the cases for quantifying the flexibility potential considering multiple rooms in a house are defined based on the interviews described above [7]. In addition to the interviews, other cases are defined to obtain insight into the flexibility potential and compare the quantified flexibility while maintaining various indoor temperatures.

With this background, the cases defined to study the flexibility potential are listed below.

- Case 1: Reduction of indoor temperature from 20 °C to 15 °C in the entire house.
- Case 2: Maintain 20 °C in the living room and turn off the heating in the other rooms.
- Case 3: Reduction of the temperature in Bedroom 2 from 20 °C to 17.5 °C and in the other rooms, the minimum acceptable temperature is set to 10 °C.
- Case 4: Uniform heating of the entire house versus heating a well-insulated smallest room (Bedroom 2) versus heating a larger room (Living room), at various temperatures ranging between 19 °C and 15 °C.

In all cases, a power deficit situation occurs at hour 6.75 in the power system that is heavily dependent on a reduction in the electric power consumption. At this time, the indoor temperatures in the house is reduced to support the power system. Later, at hour 24, the recovery of the indoor temperatures is initiated as the reserve power plants are restored.

The case study undertaken is a preprepared resilience action. The contribution from several such houses has the potential to save the power system from a disastrous event, where a black-out would be the alternative. Thus, it is unavoidable that normal indoor temperature comforts are violated. Such events happen very rarely, but give a potential of cost savings, since the option is to build out reserve power generation that, in principle, always is on stand-by.

In this study, flexibility is defined as a reduction in the electric power consumption of a heat pump, relative to the electric power consumption while maintaining 20 °C in a house.

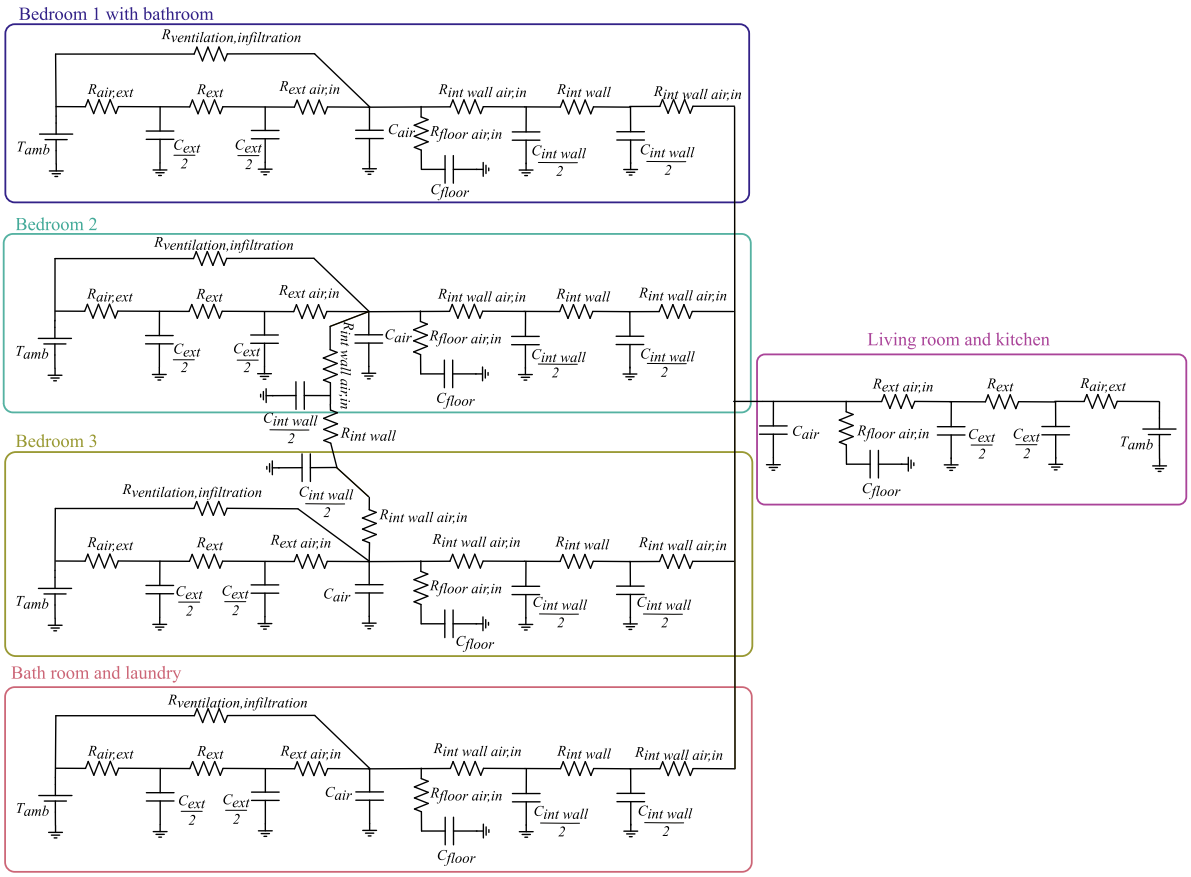

Fig. 9. Thermal model of the house.

3.5. Delimitations

The following are the delimitations of the current study:

- The indoor temperature is dependent on several factors such as solar irradiation, wind speed and activities of residents. These aspects are excluded from the thermal model of a house to eliminate uncertainty. In addition, internal and solar heat gains are relatively smaller in Swedish residential houses [31].
- Experimental validation of the models developed is not included.

4. Results and discussion

In this study, the main objective is to quantify the flexibility potential by compromising thermal comfort to various degrees in different rooms of the house considered for the analysis.

4.1. Heat pump model validation

The heat pump model under study is validated by comparing the results obtained under the standard air conditioning and refrigeration institute conditions (ARI), that is, the 7.2 °C evaporator temperature, 54.4 °C condenser temperature, with super heating of 11 °C and sub-cooling of 8.3 °C, with the data provided in [27]. The refrigerant properties at different states are taken from [32].

The results are tabulated in Table 5 and it is seen that the agreement is good. A discrepancy of 6.7% is observed in the maximum heat delivered. This might be because heat losses in the evaporator are not taken into account. However, the results of the electric power consumption from the model presented agree well with the data provided in [27].

As refrigerant R410a is phased out in the European union, a possible alternative is refrigerant R32. Under standard ARI conditions, the developed heat pump model with refrigerant R32 delivers 10.2 kW heat by consuming 2.86 kW of electric power. Thus, giving a COP of 3.57 at a compressor speed of 3240 RPM. Upon comparing this with the result in Table 5, it is observed that comparable heating power can be provided at a lower speed and electric power input when R410a is replaced by R32. This is in line with the result presented in [33]. Thus, the heat pump model developed works well.

Table 5
Comparison of result obtained with data provided in [27].

Compressor model	ZPV030	
	Data	Obtained
Speed (RPM)	3600	3600
Rated Capacity (kW) @ ARI 3600 RPM	9.7	10.35
Electric power input (kW)	2.98	2.94
Co-efficient of Performance (COP)	3.25	3.52

To further validate the heat pump model under different conditions, COP of the heat pump under study is compared with the COP of air source heat pumps with scroll compressors in [34]. The refrigerant considered in [34] is R32. As witnessed previously, there is only a slight difference in COP when using R32 and R410a. Thus, for the heat pump under study, refrigerant R410a is considered.

The COP of the air source heat pump under study with EVI operation and the COP of air source heat pumps in [34], to deliver water at 55 °C at various outdoor temperatures is shown in Fig. 10.

It is observed that the COP obtained from the heat pump model in the current study is well in agreement with the data available in [34].

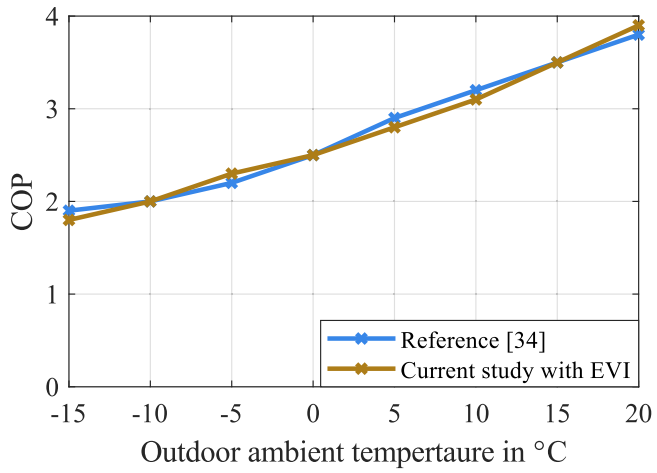

Fig. 10. COP comparison of the heat pump under study with EVI operation to deliver water at 55 °C at various outdoor temperatures, with the available data in [34].

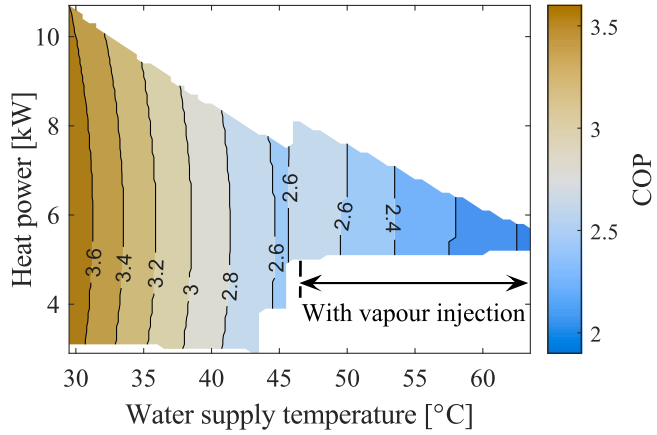

Fig. 11. Performance of the air source heat pump at an outdoor ambient temperature of −5 °C.

4.2. Performance of the air source heat pump under study

The heat delivering capacity of the air source heat pump under study, at an outdoor ambient temperature of −5 °C, is shown in Fig. 11. It is observed that as the water supply temperature increases, the heat delivered and the COP reduces. When the water supply temperature reaches the value of 46 °C, there is an increase in the heat delivering capacity and the COP value increases to 2.7. The reason for this is that to supply higher water temperatures at low outdoor temperatures, the heat pump must operate with vapour injection, as indicated in the operating envelope in Fig. 7. As a result, the performance of the heat pump improved. In addition, it is interesting to note that the minimum value of heat delivered is higher in comparison to the heat-delivering capability at low water supply temperatures.

The result on the minimum heat-delivering capability becomes important in flexibility studies. For instance, if the required heat is lower than the minimum heat provided by the heat pump, it leads to an on-off operation, like fixed-speed heat pumps even for a variable-speed heat pump.

4.3. Case 1: Reduction of indoor temperature from 20 ° C to 15 °C in the entire house.

With the objective of supporting the power system under severe power deficit conditions, the indoor temperature is allowed to reduce until 15 °C, in the house under study. This case is chosen based on the lowest acceptable thermal threshold stated in the interviews.

During normal conditions, when the indoor temperature is maintained at 20 °C throughout the house, it is observed that around 6 kW of heat is required. The corresponding electric power consumption is around 2.3 kW and the required water supply temperature is around 46 °C. This can be observed in Fig. 12(a), Fig. 12(b), Fig. 12(c) and Fig. 12(d), respectively. The corresponding COP and the speed of the heat pump are shown in Fig. 12(e).

When supporting the power system by reducing the indoor temperature to 15 °C, it is noticed that there is a period without electric power consumption for almost 8 h. Here, a flexibility of 100% is offered for a duration of 8 h.

Later, when the heating is again started to maintain the indoor temperature at 15 °C, it is observed that the heat pump turns on and off like a traditional fixed speed heat pump. This is due to the operational limitations of the heat pump. Observing Fig. 7, it is observed that the minimum speed of the heat pump corresponding to an evaporating temperature of −13 °C (the outdoor ambient temperature is −5 °C, considering 8 °C drop between the evaporator and the source, results in an evaporating temperature of −13 °C) and the condensing temperature varying between 33 °C and 36 °C is 1800 RPM. The heat delivered by the heat pump at this speed is greater than the desired value, and hence the heat pump behaves like a fixed-speed heat pump for some time. Here, the average consumption of electric power is 1.0 kW and the corresponding flexibility is reduced from 100% to 57% to maintain the indoor temperature at 15 °C.

During the recovery of indoor temperature in all rooms, it is observed that as the heating demand in the rooms increases, additional electric heating is used, as seen in Figs. 12(b) and 12(c). Consequently, the electric power consumption also increases and then gradually decreases as the target indoor temperature is achieved. In this case, the peak electric power consumption of 6 kW lasts for a duration of about 8.4 h.

It is interesting to observe that the flexibility of 100% can be offered for 8 h, with the consequence that the indoor temperature drops to 15 °C. Later, the flexibility offered gradually reduces to 57% to maintain the indoor temperature at 15 °C.

4.4. Case 2: Maintaining a warmer living room and turning off the heating in all the other rooms under study

To support the grid during severe power deficit conditions, the space heating to all the rooms except for the living room is turned off, based on the interview results. In this case, the objective is to provide heating only to the living room to maintain its temperature at 20 °C.

In Fig. 13(b) during normal operating conditions, it is observed that the heating demand is highest in the living room, followed by Bedroom 1, Laundry and bathroom, Bedroom 3 and Bedroom 2. It can be inferred that the higher the heated floor area, the greater the heating demand. However, although the area of Bedroom 2 and Bedroom 3 is the same, the heating demand is slightly lower in Bedroom 2. This is because Bedroom 2 is better insulated as its external wall area is lower compared to Bedroom 3.

During the flexibility period, when the heating is turned off in all rooms except the living room, the heating demand in the living room is observed to gradually increase to maintain the temperature at 20 °C. This is due to the drop in indoor temperature in the other rooms. As Bedroom 2 is better insulated, it takes longer for the temperature to drop compared to the other rooms.

The electric power consumption reduces to 1.2 kW for a duration of 6 h, which corresponds to a flexibility of about 48%. This value gradually reduces to about 39% due to the increase in heating demand, as the temperature is reduced in the other rooms. The average consumption of electric power during the flexibility period is 1.28 kW, which corresponds to a flexibility of 44%.

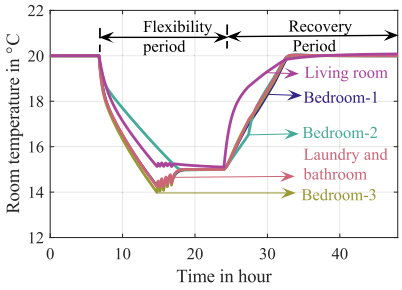

(a) Indoor temperature

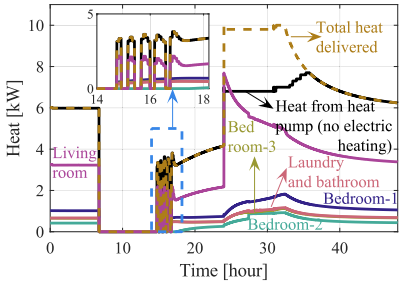

(b) Heat power consumption

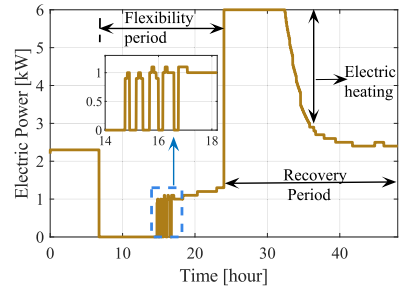

(c) Electric power consumption

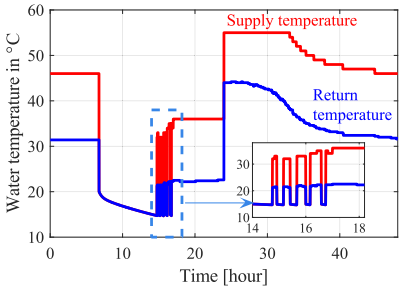

(d) Water supply and return temperature

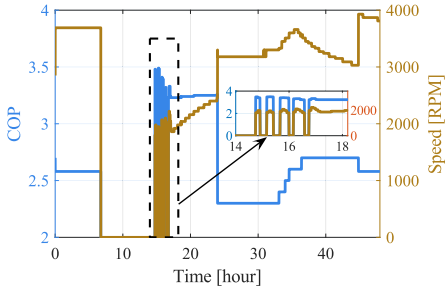

(e) COP (excluding the electric heating) and speed

Fig. 12. Thermodynamics in the house under study, equipped with the variable speed air source heat pump when reducing the indoor temperature to 15 °C in the entire house, at an outdoor ambient temperature of −5 °C.

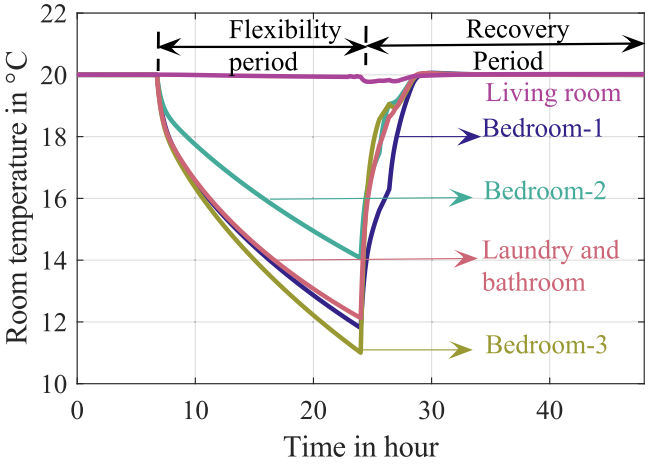

(a) Indoor temperature

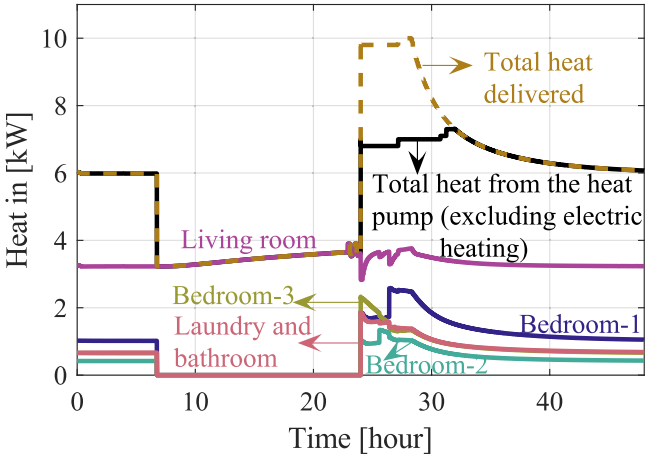

(b) Heat power consumption

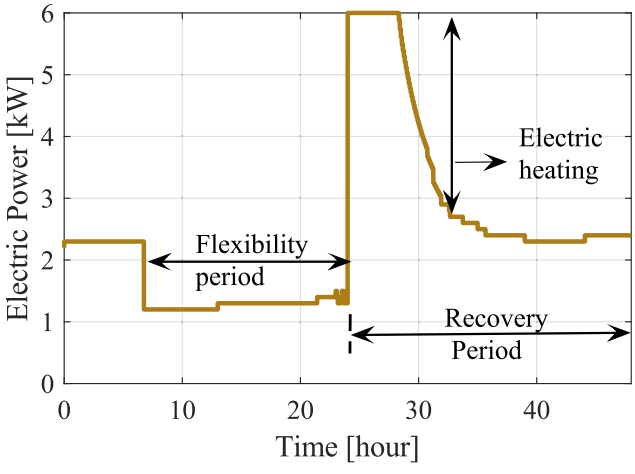

(c) Electric power consumption

Fig. 13. Thermodynamic behaviour in the house under study, equipped with the variable speed air source heat pump when maintaining 20 °C in the living room and shutting off heating in the other rooms, at an outdoor ambient temperature of −5 °C.

During the recovery period, the peak electric power consumption of 6 kW occurs for a duration of about 4.3 h and gradually reduces as the target indoor temperatures are achieved.

In this case, a flexibility of 44% is provided during the flexibility period.

4.5. Case 3: Reduction of the temperature in bedroom 2 from 20 ° C to 17.5 °C and in the other rooms, the minimum acceptable temperature is set to 10 °C

The indoor temperature of Bedroom 2 is reduced to 17.5 °C from 20 °C and in all other rooms the objective is to maintain a minimum indoor temperature of 10 °C, to support the power grid with severe power deficit conditions.

Fig. 14 shows the indoor temperatures, the heating demand in different rooms of the house, followed by the electric power consumption.

During the flexibility period, it is observed that in rooms other than Bedroom 2, the indoor temperature is not maintained at a minimum value of 10 °C. This is because the minimum value of the heat delivered by the heat pump to maintain the indoor temperature at 17.5 °C in Bedroom 2 is much higher than the desired value (between 0.25 kW and 0.4 kW). Hence, excess heat is instead delivered to other rooms to prevent the heat pump from cycling. Thus, the indoor temperatures in the other rooms are well above the value of 10 °C.

In Fig. 14(c) it is observed that there is a period without electric power consumption for five hours. Thus, a flexibility of 100% can be provided for five hours. Later, the flexibility reduces to 57%, as heating is required to maintain the indoor temperature of Bedroom 2 at 17.5 °C.

During the recovery of indoor temperatures to 20 °C, it is observed that the peak electric power consumption of 6 kW lasts for a duration of 7.74 h.

In this case, a flexibility of 100% can be offered for 5 h. After 5 h, the flexibility offered is reduced to 57%.

4.6. Case 4: Summary of results from uniform heating of the entire house versus heating a well-insulated smallest room versus heating a larger room, to various temperatures ranging between 19 ° C and 15 °C

The main objective of this article is to investigate and quantify the flexibility provided by a house equipped with a heat pump by maintaining different temperatures in various rooms of the house. Hence, flexibility is quantified by comparing three scenarios: uniformly heating the entire house to the same temperature, heating a well-insulated smallest room, and heating a larger room to various temperatures ranging between 19 °C and 15 °C, during the time of resiliency activation.

The consolidated results of flexibility offered in the above cases by reducing the indoor temperatures from 20 ° C and keeping them between 19 °C and 15 °C is shown in Fig. 15. Fig. 15(a) shows the duration for which a flexibility of 100% can be provided, or, in other words, the duration without any electric power consumption due to thermal inertia of the house. As anticipated, the greater the thermal compromise, the longer the duration for which 100% flexibility can be provided. It is observed that by only heating a well-insulated small room, 100% flexibility can be provided for a longer duration compared to the other two cases. Furthermore, a flexibility of 100% can be provided for a similar duration while maintaining better thermal comfort in the well-insulated small room compared to the other two cases.

For example, a flexibility of 100% is provided for 5 h, with the consequence that the thermal comfort in all rooms of the house drop to about 16 °C, at an outdoor temperature of −5 °C. The same flexibility is provided by heating only a smaller area such as the better insulated Bedroom 2, which is 8% of the total floor area, to 17.5 °C, while ensuring that the temperatures in the other rooms do not fall below 14 °C as seen in Fig. 14.

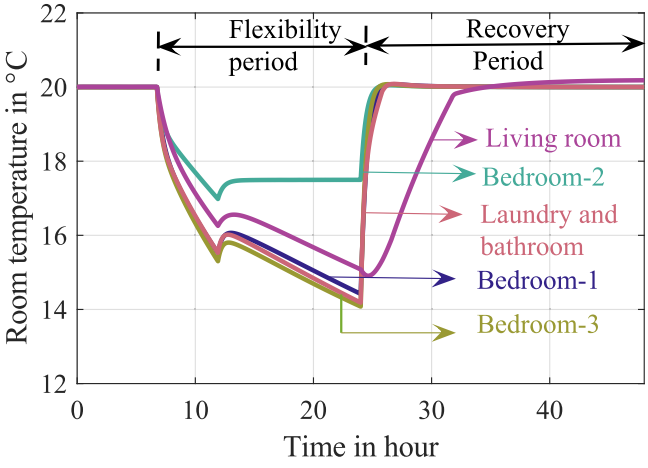

(a) Indoor temperature

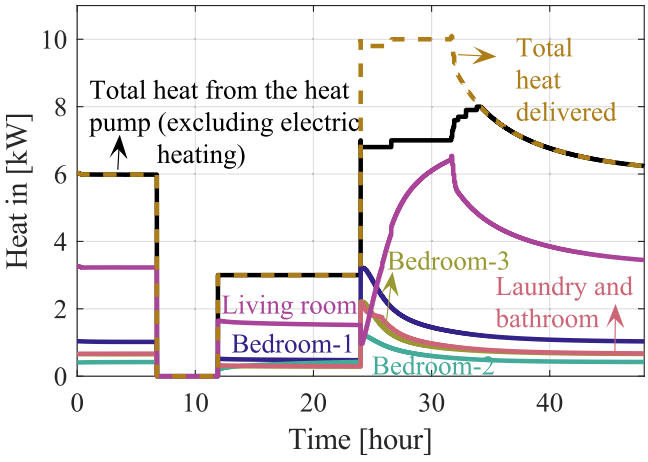

(b) Heat power consumption

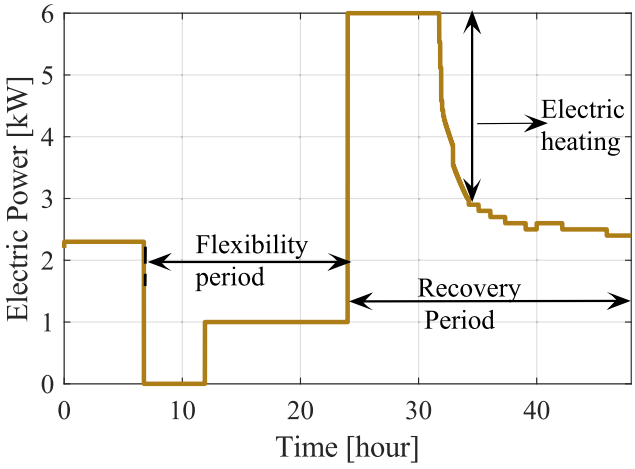

(c) Electric power consumption

Fig. 14. Thermodynamic behaviour in the house under study, equipped with the variable speed air source heat pump when maintaining 17.5 °C in the smallest well insulated room, at an outdoor ambient temperature of −5 °C.

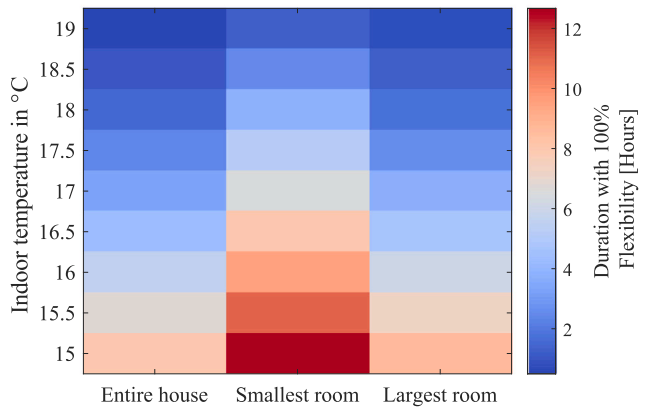

(a) Duration for which 100% flexibility is provided

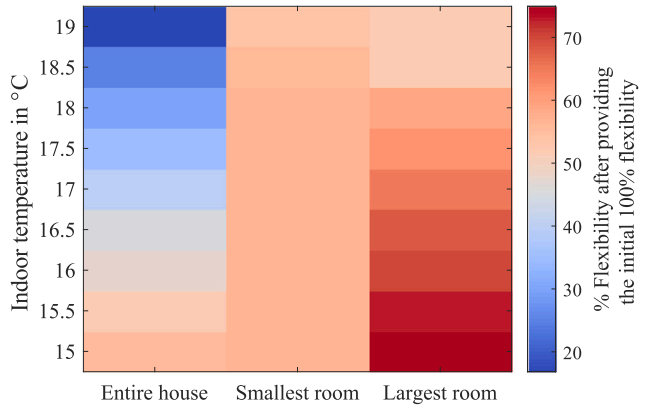

(b) Final flexibility after providing an initial flexibility of 100%

Fig. 15. Flexibility quantification while maintaining different temperatures in various rooms of a house, at an outdoor ambient temperature of −5 °C.

After some hours (as presented in Fig. 15(a)) the flexibility reduces from 100%, as the indoor temperatures is to be maintained at specified minimum values. The change in flexibility from 100% to various values in different cases is shown in Fig. 15(b). Here, it is observed that the flexibility level looks the same for different temperature reductions in the smallest room, which is Bedroom 2. This is because the minimum value of the heat delivered by the heat pump is much higher than the desired heating requirements in Bedroom 2, as seen in Section 4.5. As a result, excess heat is delivered to other rooms. Consequently, the flexibility levels (electric power reduction) looks the same for various degrees of thermal compromise in Bedroom 2. For the other cases, it is inferred that the greater the degree of thermal compromise, the greater the flexibility provided.

Individual's preference or acceptance of personal comfort has a great impact on the flexibility provision from the house. The advantage of such a flexible resource is that the aggregated flexibility of multiple houses can be reshaped to a desired profile at the system level.

4.7. Validation of the building's thermal model

Based on the building parameters described in Section 3.2, the overall heat transfer coefficient (thermal resistances to outdoor temperature) of the house, including infiltration losses and heat recovery, is calculated to be 239.23 $\left(\frac{\mathrm{W}}{\mathrm{K}}\right)$.

Using the overall heat transfer coefficient, the heat required to maintain an indoor temperature of 20 °C at an outdoor ambient temperature of −5 ° C is estimated to be 5.98 kW. Here, the proportion of heat losses due to mechanical ventilation including heat recovery in each room can be calculated using (10), by neglecting infiltration. This is estimated to be 537 W, which is about 9% of the total heat demand in the house.

When 20 °C is maintained throughout the house, there is no heat transfer between adjacent rooms. Thus, the heat requirement in each room can be estimated by calculating the heat transfer coefficient of each room with respect to the outdoor temperature. For each room this can be calculated by determining the thermal equivalent of the parallel combination of ($R_{ventilation,infiltration}$) with ($R_{air,ext}$ + R_{ext} + $R_{ext\ air,in}$). These values are estimated to be 1.02 kW, 0.42 kW and 0.65 kW for Bedroom-1, Bedroom-2, and Bedroom-3, respectively. Furthermore, for the living room followed by the laundry and bathroom, the heat requirements are estimated to be 3.23 kW and 0.67 kW, respectively. The total heat requirement in the house under study would be the summation of the heat requirement in each room and is estimated to be 5.99 kW. The total heat requirement and the heat requirement in each room to maintain 20 °C at an outdoor ambient temperature of −5 °C are well matched with the values obtained in the above three case studies, as seen in Figs. 12(b), 13(b) and 14(b). Thus, the thermal model of the house works as desired.

4.8. Simulation set up, solver specification and performance parameters

The developed model was simulated in MATLAB Simulink using an automatic solver and a 30-second time step. The computation time for each simulation is 39.3 s. The computer used for simulation is equipped with 64 GB RAM, Intel® Core™ i9-10900 CPU @ 2.80 GHz, 10 cores.

5. Conclusion

This article demonstrated the ability of single-family houses equipped with heat pumps to be used as flexible resources to support the power system in situations of severe power shortages.

In order to investigate the flexibility potential of maintaining different temperatures in various rooms of a house, a detailed model of a multi-room Swedish single-family house equipped with a variable-speed heat pump was developed. The model also includes the space heating controller to control the temperatures in different rooms of a house.

An initial indoor temperature of 20 °C is considered for the analysis in all rooms and an outdoor ambient temperature of −5 °C. In this study, flexibility is defined as a reduction in the electric power consumption of a heat pump, relative to the electric power consumption while maintaining 20 °C in a house.

A flexibility of 100% is provided for 5 h, when all rooms reduce thermal comfort equally to about 16 °C, at an outdoor temperature of −5 °C. The same flexibility can also be provided by heating only a smaller area, such as a better insulated bedroom, which is 8% of the total floor area, to 17.5 °C, while ensuring that the temperatures in the other rooms do not fall below 10 °C. After the first five hours, the flexibility decreases from 100% to 47% and 57%, respectively, in the above cases, for as long as the flexibility required. The impact of offering various levels of flexibility in relation to thermal comfort is demonstrated and quantified in this article.

CRediT authorship contribution statement

Sindhu Kanya Nalini Ramakrishna: Writing – review & editing, Writing – original draft, Visualization, Validation, Methodology, Investigation, Formal analysis, Data curation, Conceptualization. **Torbjörn Thiringer:** Writing – review & editing, Supervision, Resources, Project administration, Funding acquisition, Conceptualization. **Peiyuan Chen:** Writing – review & editing, Supervision.

Declaration of competing interest

The authors declare that they have no known competing financial interests or personal relationships that could have appeared to influence the work reported in this paper.

Acknowledgement

The financial support provided by the Swedish Energy Agency through grant No. 50343-1 is gratefully acknowledged.

Data availability

Data will be made available on request.

References

[1] Große C, Olausson PM. Is there enough power? Swedish risk governance and emergency response planning in case of a power shortage. 2025, [Online]. Available: URL https://snsse.cdn.triggerfish.cloud/uploads/2023/01/is-there-enough-power.pdf. [Accessed 13 June 2025].

[2] Emergency information from Swedish authorities. Reserve power and the "styrel" system. 2025, [Online]. Available: URL https://www.krisinformation.se/en/hazards-and-risks/power-outages/reserve-power-and-the-styrel-system. [Accessed 13 June 2025].

[3] Swedish Energy Agency. Energy in Sweden- an overview. Energimyndigheten; 2021.

[4] statista. Final electricity consumption in households in Sweden from 2013 to 2019, by type. 2021, [Online]. Available: https://Www.Statista.Com/Statistics/1027100/Final-Consumption-of-Electricity-in-Households-in-Sweden-By-Type/.

[5] Chen H, Ruud S, Markusson C. Energy flexibility using thermal mass for Swedish single-family houses. In: E3S web of conf., vol. 562, 2024, p. 04003.

[6] Walfridson T, Lindahl M, Ericsson N, Bergentz T, Willis M, Gustafsson O, Haglund Stignor C. Large scale demand response of heat pumps to support the national power system. In: 14^{th} IEA, heat pump conference. 2023.

[7] Nalini Ramakrishna SK, Björner Brauer H, Thiringer T, Håkansson M. Social and technical potential of single family houses in increasing the resilience of the power grid during severe disturbances. Energy Convers Manage 2024;321:119077, [Online]. Available: URL https://www.sciencedirect.com/science/article/pii/S0196890424010185.

[8] Johnson R, Royapoor M, Mayfield M. A multi-zone, fast solving, rapidly reconfigurable building and electrified heating system model for generation of control dependent heat pump power demand profiles. Appl Energy 2021;304:117663, [Online]. Available: URL https://www.sciencedirect.com/science/article/pii/S0306261921010266.

[9] Khatibi M, Rahnama S, Vogler-Finck P, Dimon Bendtsen J, Afshari A. Towards designing an aggregator to activate the energy flexibility of multi-zone buildings using a hierarchical model-based scheme. Appl Energy 2023;333:120562, [Online]. Available: URL https://www.sciencedirect.com/science/article/pii/S0306261922018190.

[10] Golmohamadi H, Guldstrand Larsen K, Gjøl Jensen P, Riaz Hasrat I. Optimization of power-to-heat flexibility for residential buildings in response to day-ahead electricity price. Energy Build 2021;232:110665, [Online]. Available: URL https://www.sciencedirect.com/science/article/pii/S0378778820334514.

[11] Golmohamadi H, Larsen KG, Jensen PG, Hasrat IR. Hierarchical flexibility potentials of residential buildings with responsive heat pumps: A case study of Denmark. J Build Eng 2021;41:102425, [Online]. Available: URL https://www.sciencedirect.com/science/article/pii/S2352710221002825.

[12] Clauß J, Stinner S, Sartori I, Georges L. Predictive rule-based control to activate the energy flexibility of Norwegian residential buildings: Case of an air-source heat pump and direct electric heating. Appl Energy 2019;237:500–18, [Online]. Available: URL https://www.sciencedirect.com/science/article/pii/S0306261918318932.

[13] Saleem A, Ugalde-Loo CE. Thermal performance analysis of a heat pump-based energy system to meet heating and cooling demand of residential buildings. Appl Energy 2025;383:125306, [Online]. Available: URL https://www.sciencedirect.com/science/article/pii/S0306261925000364.

[14] Hua P, Wang H, Xie Z, Lahdelma R. Integrated demand response method for heating multiple rooms based on fuzzy logic considering dynamic price. Energy 2024;307:132577, [Online]. Available: URL https://www.sciencedirect.com/science/article/pii/S036054422402351X.

[15] Biyik E, Kahraman A. A predictive control strategy for optimal management of peak load, thermal comfort, energy storage and renewables in multi-zone buildings. J Build Eng 2019;25:100826, [Online]. Available: URL https://www.sciencedirect.com/science/article/pii/S2352710219302165.

[16] Langner F, Frahm M, Wang W, Matthes J, Hagenmeyer V. Hierarchical-stochastic model predictive control for a grid-interactive multi-zone residential building with distributed energy resources. J Build Eng 2024;89:109401, [Online]. Available: URL https://www.sciencedirect.com/science/article/pii/S2352710224009690.

[17] Frahm M, Dengiz T, Zwickel P, Maaß H, Matthes J, Hagenmeyer V. Occupant-oriented demand response with multi-zone thermal building control. Appl Energy 2023;347:121454, [Online]. Available: URL https://www.sciencedirect.com/science/article/pii/S0306261923008188.

[18] Verdugo P, Cañizares C, Pirnia M. Modeling and energy management of hangar thermo-electrical microgrid for electric plane charging considering multiple zones and resources. Appl Energy 2025;379:124951, [Online]. Available: URL https://www.sciencedirect.com/science/article/pii/S0306261924023341.

[19] Air Squared Articles. Scroll compressor and vaccum pump efficiency. [Online]. Available: URL https://airsquared.com/scroll-articles/scroll-compressor-and-scroll-vacuum-pump-efficiency-explained/.

[20] Nalini Ramakrishna SK, Thiringer T, Markusson C. Quantification of electrical load flexibility offered by an air to water heat pump equipped single-family residential building in Sweden. In: 14^{th} IEA, heat pump conference. 2023.

[21] Emerson Climate Technologies. Economized vapor injection (EVI) for ZF*KVE and ZF*K5E compressors. In: Application engineering bulletin. Emerson Climate Technologies; 2019, p. 1–29, [Online]. Available: URL https://manuals.plus/m/e818094ec40575e210f4978adde1dcd6155b6106777404e3c388e2f1dc184096.pdf.

[22] Emerson Climate Technologies. Scroll compressors with vapour injection for dedicated heat pumps. In: Application guidelines. Emerson Electric Co.; 2004, [Accessed 04 March 2022].

[23] Nalini Ramakrishna SK, Thiringer T. Modelling of heat pumps, controller for space and water heating. Technical report, chalmers university of technology, gothenburg, 2024; 2024.

[24] Kuniyoshi R, Kramer M, Lindauer M. Validation of RC building models for applications in energy and demand side management. In: Proceedings of eSim 2018. IBPSA Canada; 2018, p. 1–2–B–4, [Online]. Available: URL https://publications.ibpsa.org/proceedings/esim/2018/papers/esim2018_1-2-B-4.pdf.

[25] Johra H, Heiselberg P. Influence of internal thermal mass on the indoor thermal dynamics and integration of phase change materials in furniture for building energy storage: A review. Renew Sustain Energy Rev 2017;69:19–32, [Online]. Available: URL https://www.sciencedirect.com/science/article/pii/S1364032116309042.

[26] Hong T, Lee SH. Integrating physics-based models with sensor data: An inverse modeling approach. Build Environ 2019;154:23–31, [Online]. Available: URL https://www.sciencedirect.com/science/article/pii/S036013231930160X.

[27] Emerson. Copeland™ scroll. In: Variable speed compressors for residential air conditioning applications. Emerson Electric Co.; 2020, [Accessed 04 March 2022].

[28] Haglund Stignor C, Walfridson T. Nordsyn study on air-to-water heat pumps in humid nordic climate. In: Nordic council of ministers. 2019.

[29] Vadiee A, Dodoo A, Jalilzadehazhari E. Heat supply comparison in a single-family house with radiator and floor heating systems. Buildings 2020;10(1). [Online]. Available: URL https://www.mdpi.com/2075-5309/10/1/5.

[30] Blom N. Folkhälsomyndighetens allmänna råd om temperatur inomhus. Folkhälsomyndigheten; 2014.

[31] Mata E, Kalagasidis AS. In: Calculation of energy use in the Swedish housing, vol. 2009, Gothenburg, Sweden: Chalmers Univeristy of Technology; 2009, p. 4.

[32] Bell IH, Wronski J, Quoilin S, Lemort V. Pure and pseudo-pure fluid thermophysical property evaluation and the open-source thermophysical property library CoolProp. Ind Eng Chem Res 2014;53(6):2498–508, [Online]. Available: URL http://pubs.acs.org/doi/abs/10.1021/ie4033999.

[33] Zaman MA, Wang S. Effects of refrigerant drop-in (R32/R410) on the performance of a heat pump system. In: International refrigeration and air conditioning conference. 2024, [Online]. Available: URL https://docs.lib.purdue.edu/iracc/2622.

[34] Olympios AV, Song J, Ziolkowski A, Shanmugam VS, Markides CN. Data-driven compressor performance maps and cost correlations for small-scale heat-pumping applications. Energy 2024;291:130171, [Online]. Available: URL https://www.sciencedirect.com/science/article/pii/S036054422303565X.